SUPPLEMENTARY INFORMATION

SUPPLEMENTARY FIGURES

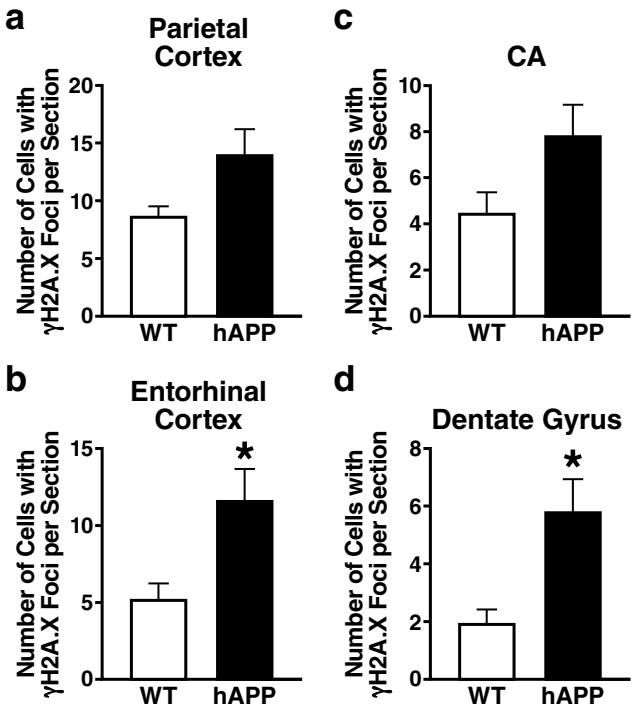

Supplementary Figure 1. Increased number of neurons with γH2A.X foci in young hAPP-J20 mice

(a-d) Numbers of cells with γH2A.X-positive foci in different brain regions of 1.5–2.2-month-old NTG and hAPP-J20 mice (n=6 mice/genotype). *p<0.05 (two-tailed, unpaired Student's *t*-test). Bars represent means ± SEM.

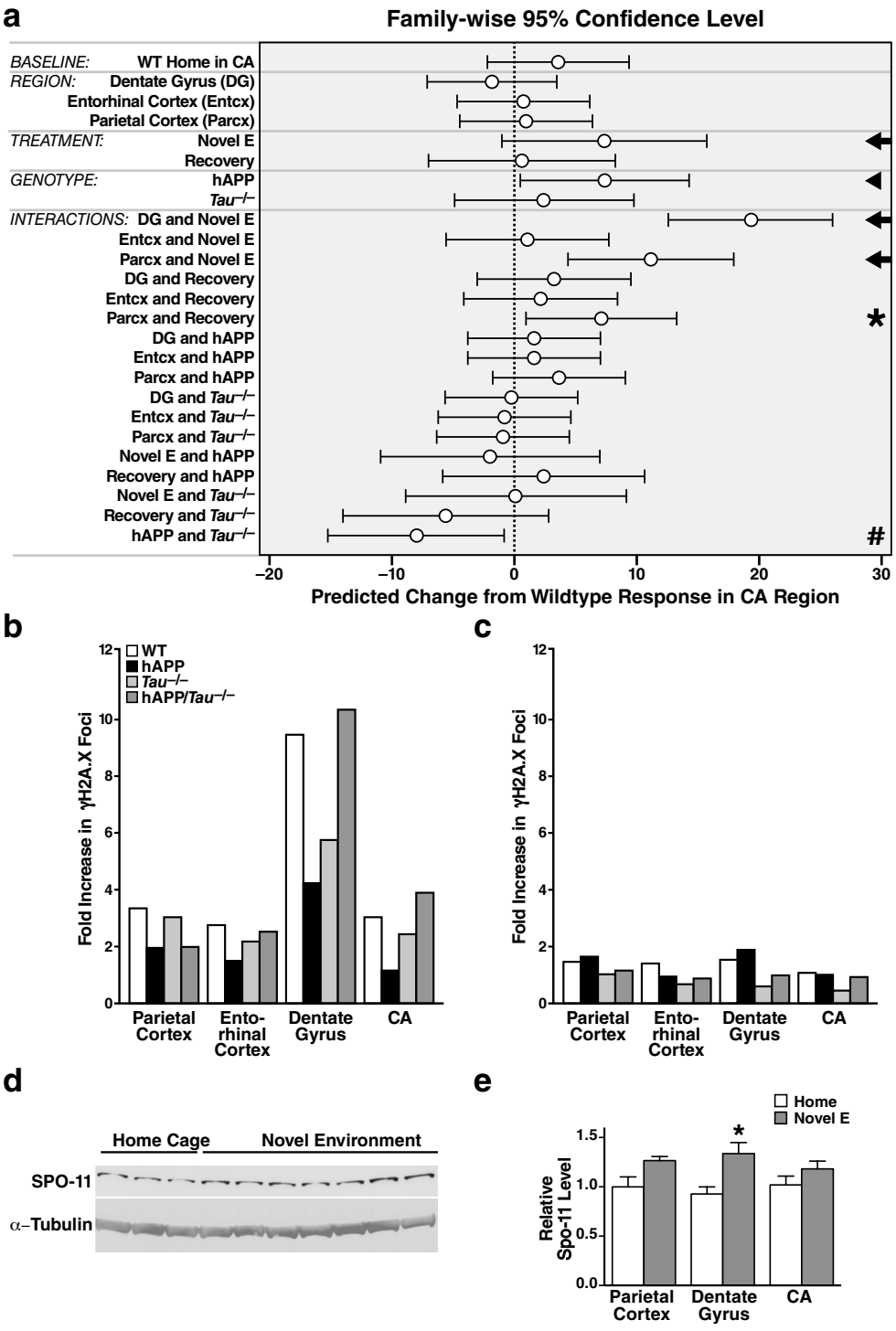

Supplementary Figure 2. Complementary analysis of data presented in Figure 2

(a) The factor level and interaction effects of behavioral treatment (Control, Novel E, and Recovery) and genotype (*Tau*$^{+/+}$, *Tau*$^{-/-}$, hAPP/*Tau*$^{+/+}$, and hAPP/*Tau*$^{-/-}$) on the number of neurons with γH2A.X-positive foci in different brain regions were estimated by a linear model with a random effect, to account for repeated measures from the brains of the

same mice. CA, hippocampal CA region; DG, dentate gyrus; Entcx, entorhinal cortex; Parcx, parietal cortex. The model consists of main effects and two-way interaction terms; there was insufficient power to detect higher-order interactions with this model. The reference level estimate in the CA region of wildtype mice in the control home cage condition is shown at the top, followed by the estimated effects of changes in specified treatment, genotype, or region. The confidence intervals shown represent 95% family wise–adjusted confidence intervals. The four-way repeated ANOVA for this model indicated significant differences in the number of neurons with γH2A.X-positive foci among behavioral treatments ($p = 0.0228$) and between the *Tau*$^{+/+}$ and hAPP/*Tau*$^{+/+}$ genotypes ($p = 0.0018$), and in the effect of behavioral treatments on different brain regions ($p<0.0001$), as well as an interaction between the hAPP and *Tau* genotypes ($p=0.0012$). The most notable effects are denoted with a symbol on the right. Mice with hAPP had a significant overall increase in the number of neurons with γH2A.X foci (arrowhead), except when found in combination with the *Tau*$^{-/-}$ genotype; this interaction effect is denoted with a pound sign. The novel environment treatment had a strong effect on the number of neurons with γH2A.X foci in the dentate gyrus and parietal cortex, indicated by arrows. There was no statistically significant difference in the number of γH2A.X neurons between the behavioral control group and the recovery group (matching regions and genotypes), except in the parietal cortex, which had a higher number of γH2A.X neurons in the latter group (asterisk). (**b, c)** Fold changes in the number of neurons with γH2A.X foci after exploration of a novel environment **(b)** and the recovery phase **(c)**, as compared with baseline levels in the control group. Bars represent ratios between the means of the groups compared. **(d, e)** Western blot analysis of SPO-11 levels in the dentate gyrus of wildtype mice. **(d)** Representative western blot of protein extracts from the dentate gyrus of wildtype mice labeled with an antibody against SPO-11. α-Tubulin served as a loading control. Each lane contained a sample from a different mouse. **(e)** SPO-11 levels were quantitated in three brain regions of wildtype mice that had remained in their home cage or explored a novel environment for 2 h. n=4-9 mice per condition. *$p<0.05$ vs. Home (unpaired 2-tailed t-test). Bars represent means ± SEM.

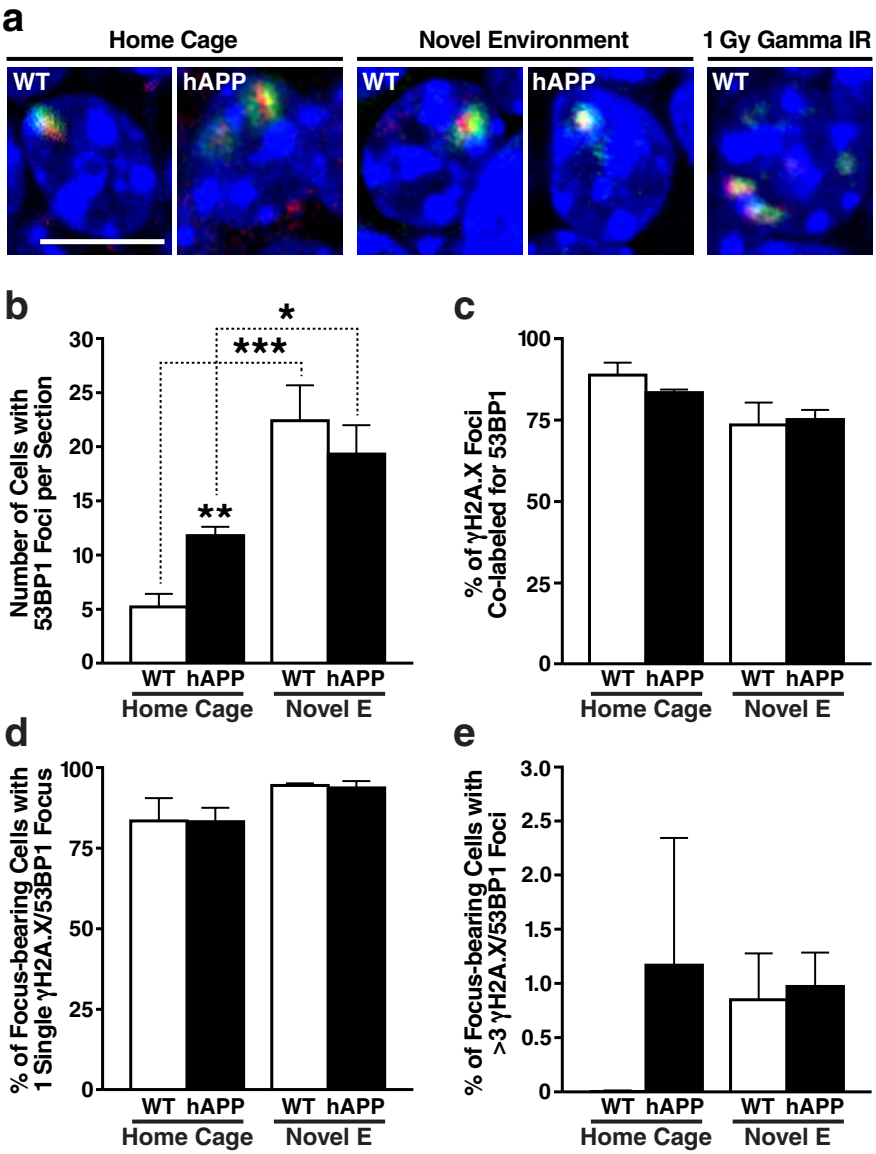

Supplementary Figure 3. Co-localization of γH2A.X and 53BP1 in nuclear foci and quantitation of foci after exploration of a novel environment

Brain sections from the dentate gyrus of 6-month-old wildtype and hAPP-J20 mice exposed to their home cage or to a novel environment for 2 h (Novel E) (Figure 3) were co-labeled with DAPI (blue) and antibodies to γH2A.X (green) and 53BP1 (red) and imaged by confocal microscopy. **(a)** Focus-bearing neuronal nuclei showed co-localization of γH2A.X and 53BP1 at individual foci, which were of roughly comparable sizes across genotypes and conditions. The rightmost micrograph shows γH2A.X foci in neuronal nuclei of a γ-irradiated (1 Gy) mouse for comparison. Scale bar: 10 μm. **(b–e)** The average number of cells bearing foci per section was determined from three

sections per mouse in 4–6 mice per genotype and condition (from 2 independent experiments). **(b)** Number of cells bearing one or more 53BP1-positive foci. **(c)** Percentage of γH2A.X foci co-labeled with anti-53BP1. **(d,e)** Percentage of focus-bearing cells with only 1 **(d)** or >3 **(e)** γH2A.X/53BP1-positive foci. *p<0.05, **p<0.01, ***p<0.0001 as indicated by brackets (Bonferroni *post-hoc* test). Two-way ANOVA revealed an effect of behavioral condition (p<0.01) in **(c),** which may reflect the formation of new DSBs during exploration that first attract γH2A.X, and only subsequently and with some delay 53BP1[1]. All other differences were not statistically significant. Bars represent means ± SEM.

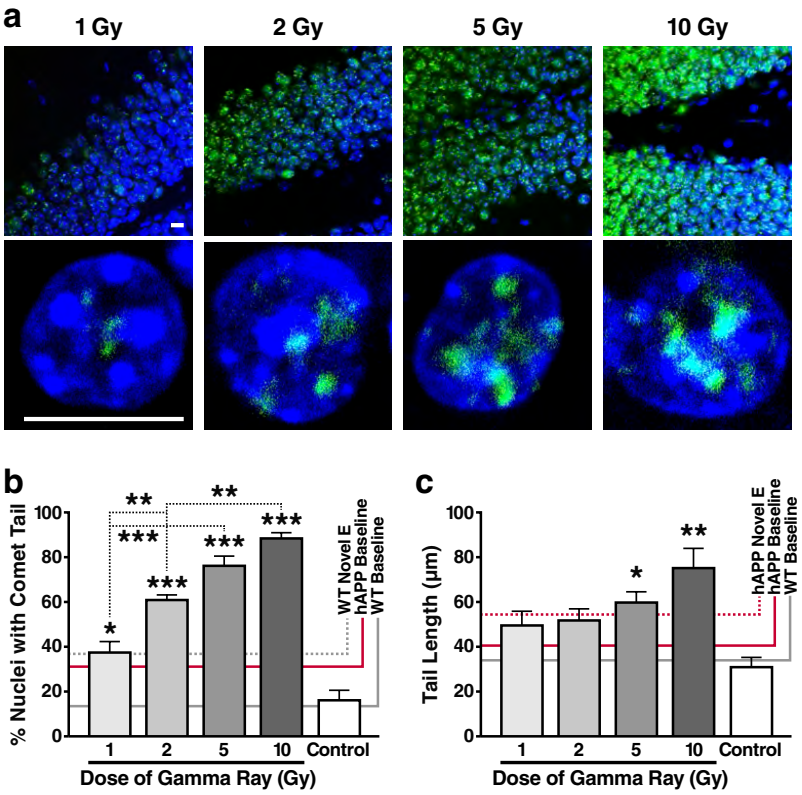

Supplementary Figure 4. Evidence for neuronal DSBs in γ-irradiated wildtype mice

After receiving 0 (control, Ctrl), 1, 2, 5 or 10 Gray (Gy) of whole-body γ-irradiation, 4–5-month-old wildtype mice were put back into their home cage for 1 h and then analyzed for neuronal DSBs in the dentate gyrus by γH2A.X immunohistochemistry **(a)** or comet assay at neutral pH **(b, c). (a)** Representative confocal micrographs showing DAPI-labeled nuclei in blue and γH2A.X-positive foci in green. Scale bar: 10 µm. **(b)** Percentage of cells with comet tails. For each mouse, 600-800 cells within 3 fields were inspected and scored. n=4 mice per dose. **(c)** Average length (in µm) of comet tails among comet-bearing cells (see also Figure 3). *p<0.05, **p<0.01, ***p<0.001 vs. rightmost bar (Dunnett's test) or as indicated by brackets (Tukey-Kramer test). Bars represent means ± SEM.

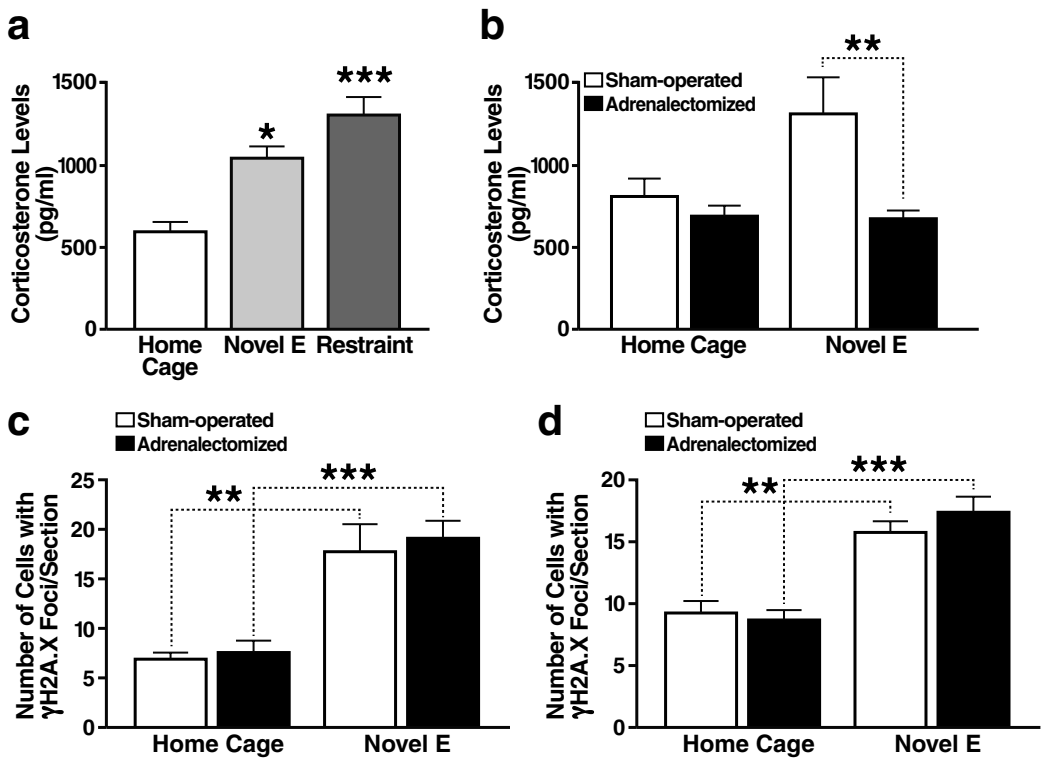

Supplementary Figure 5. Exploration-induced neuronal γH2A.X foci are not caused by stress responses

(a,b) Plasma corticosterone levels in non-operated wildtype mice **(a)** and in sham-operated versus adrenalectomized (ADX) wildtype mice **(b)** immediately after exposure to one of three conditions: (1) home cage, (2) exploration of a novel environment (Novel E) for 15 min **(a)** or 2 h **(b-d),** or (3) restraint stress (Restraint) for 15 min. Corticosterone levels in ADX mice were stress-independent and held constant through release from a subcutaneously implanted corticosterone pellet. **(c,d)** Numbers of cells with γH2A.X-positive foci in the dentate gyrus **(c)** and CA1-3 regions **(d)** of the hippocampus in sham-operated versus ADX wildtype mice. Exploration of a novel environment caused a comparable increase in the number of cells with γH2A.X foci in ADX and sham-operated mice despite their different corticosterone levels **(b).** Two-way ANOVA revealed an effect of behavioral condition ($p<0.0001$) in **(c)** and **(d)**. All mice were 8 weeks of age. n=5–7 mice per group, except for restraint-stressed ADX mice (n=3). *$p<0.05$, **$p<0.01$, ***$p<0.0001$ vs. leftmost bar (Dunnett's test) or as indicated by brackets (Bonferroni *post-hoc* test). Bars represent means ± SEM.

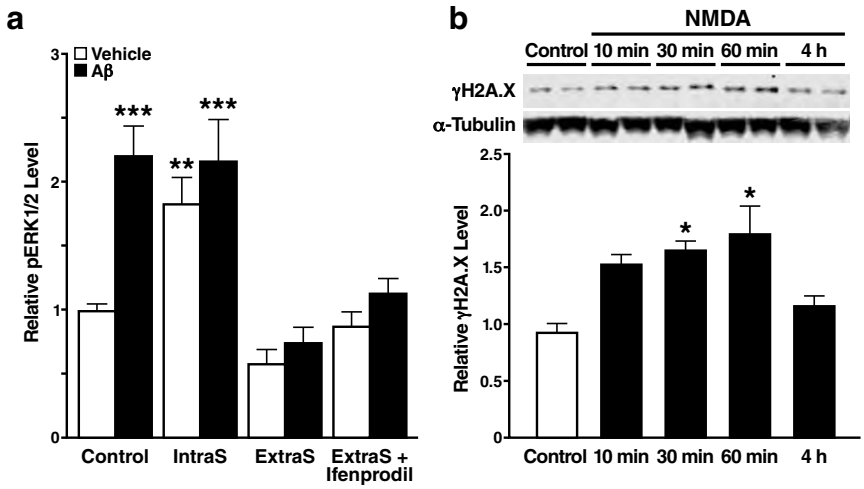

Supplementary Figure 6. γH2A.X and pERK1/2 levels increase in response to stimulation of NMDA receptors in neuronal cultures

(a) Levels of pERK1/2 were quantitatively determined by western blot analysis in primary forebrain neurons 5 h after treatment as indicated in Figure 4a. n=5–12 wells per condition from 7 independent cultures. **(b)** γH2A.X levels transiently increased in neurons after NMDA stimulation. Representative western blot (top) and quantitative analysis (bottom) of wildtype mouse primary forebrain neuronal cultures treated for 5 min with NMDA (10 μM). After a rinse, cells were incubated for 10, 30, or 60 min or 4 h in fresh medium followed by western blot analysis of γH2A.X levels. *p<0.05, **p<0.01, ***p<0.001 vs. first bar (Dunnett's *post-hoc* test). Bars represent means ± SEM.

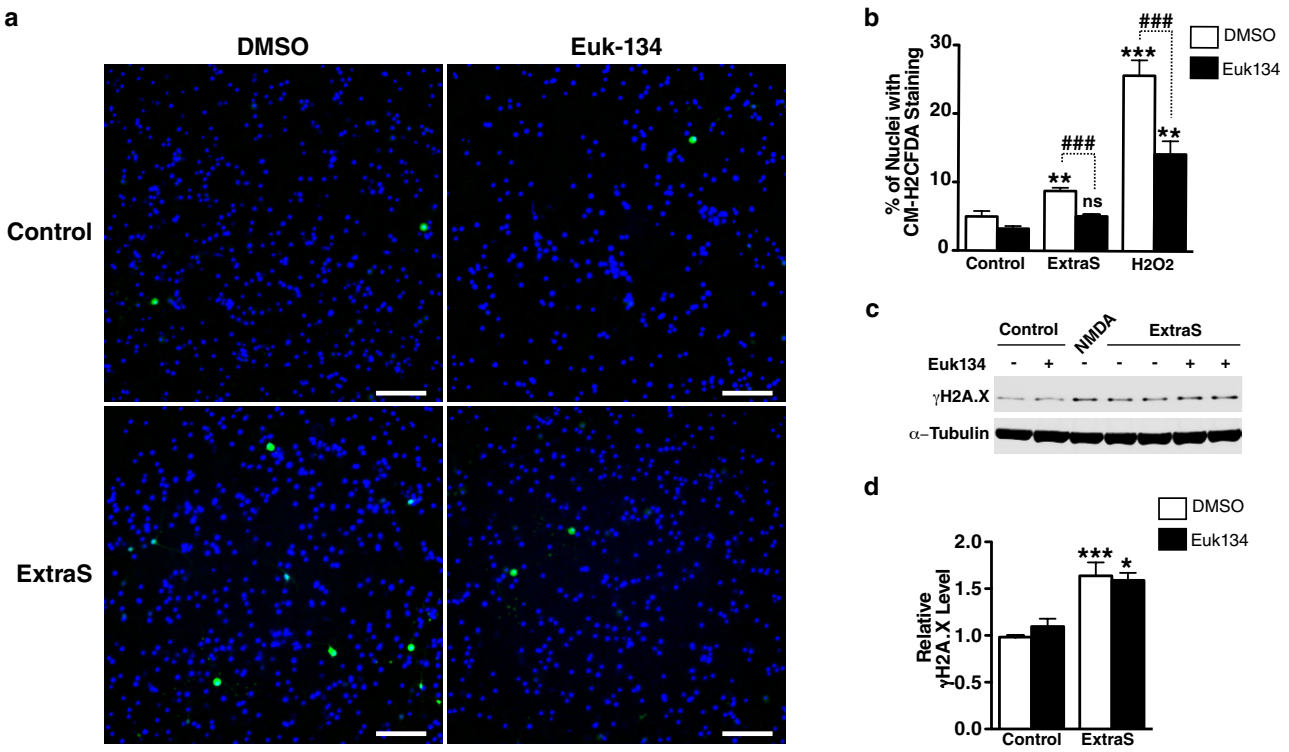

Supplementary Figure 7. Reduction of activity-induced reactive oxygen species (ROS) does not diminish activity-induced increases in neuronal γH2A.X levels

Wildtype mouse primary hippocampal neurons grown on coverslips were pre-treated for 1 h with the ROS scavenger Euk 134[2, 3] (20 mM) or vehicle (DMSO), followed by the treatments indicated in Figure 8a. One and a half hour after the end of these treatments, the ROS indicator CM-H2CFDA was added. Forty min later, the coverslips were washed with tyrode buffer and analyzed by fluorescence microscopy (a, b). Replicate cultures were lysed 2 h after the last step of the treatments and analyzed by western blotting (c–e). **(a)** Representative photomicrographs showing Hoechst 33342-labeled nuclei in blue and CM-H2CFDA-labeled nuclei in green. Scale bar: 100 μm. **(b)** Percentage of cells with CM-H2CFDA-labeled nuclei. Treatment of cultures with H_2O_2 served as a positive control. For each condition, 600-900 nuclei in 3-4 fields distributed across two culture wells were inspected for CM-H2CFDA labeling. **(c)** Representative western blot. **(d)** Quantitation of western blot signals for γH2A.X levels. n=7-8 wells per condition from 7 independent experiments. Note that in the presence of Euk134, extrasynaptic stimulation did not increase the proportion of CM-H2CFDA-positive neurons (b) but did increase the levels of γH2A.X (d). *p<0.05, **p<0.01, ***p<0.001 vs. similarly treated control (Dunnett test in b, Dunn test in d); ###p<0.001 as indicated by brackets (Bonferroni *post-hoc* test in b). Bars represent means ± SEM.

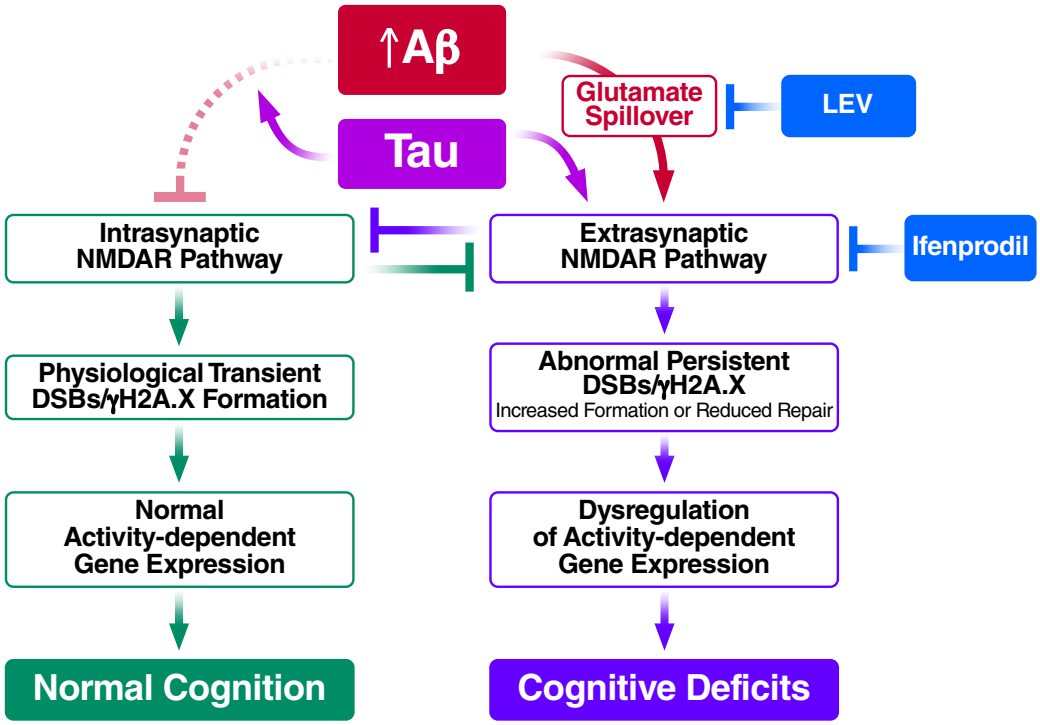

Supplementary Figure 8. Hypothetical model

At normal levels of Aβ, the physiological balance between intrasynaptic and extrasynaptic NMDAR activation promotes normal cognition. This process involves the transient formation of neuronal DSBs and γH2A.X foci, which might have a role in activity-dependent gene expression. Pathologically elevated levels of Aβ tip this balance toward overactivation of extrasynaptic NMDARs, leading to abnormal increases and persistence of neuronal DSBs and γH2A.X foci, dysregulation of activity-dependent gene expression and cognitive deficits. These pathogenic effects of Aβ depend on the presence of wildtype tau and can be blocked by drugs that lower glutamate levels around the synaptic cleft or block NR2B-containing NMDARs.

References

1. Ward, I.M., Minn, K., Jorda, K.G. & Chen, J. Accumulation of checkpoint protein 53BP1 at DNA breaks involves its binding to phosphorylated histone H2AX. *J. Biol. Chem.* **278**, 19579–19582 (2003).

2. Pong, K., Doctrow, S.R., Huffman, K., Adinolfi, C.A. & Baudry, M. Attenuation of staurosporine-induced apoptosis, oxidative stress, and mitochondrial dysfunction by synthetic superoxide dismutase and catalase mimetics, in cultured cortical neurons. *Exp. Neurol.* **171**, 84–97 (2001).

3. Rong, Y., Doctrow, S.R., Tocco, G. & Baudry, M. EUK-134, a synthetic superoxide dismutase and catalase mimetic, prevents oxidative stress and attenuates kainate-induced neuropathology. *Proc. Natl. Acad. Sci. USA* **96**, 9897–9902 (1999).